Applied Physics B (2021) 127:114
https://doi.org/10.1007/s00340-021-07661-2

Applied Physics B
Lasers and Optics

Combined photothermal lens and photothermal mirror Z-scan of semiconductors

Aristides Marcano Olaizola[1] · **José Luis Luna Sánchez**[1,2]

Received: 23 November 2020 / Accepted: 20 June 2021 / Published online: 15 July 2021

Abstract
We perform thermal lens and thermal mirror Z-scan experiments to study the photothermal properties of semiconductors. We fix the sample's position, facilitating the alignment procedure and the experiment's interpretation. By scanning the lens, which focuses the pump beam, we obtain the Z-scan signature. A diode laser at 1064 nm provides the probe beam for the thermal lens experiment, while a Helium–Neon laser generates it for the photothermal mirror one. Using a telescope, we collimated the probe beam having a nearly constant radius of few millimeters. In this configuration, the z-scan response is single peaked. We fit both experimental results using a model based on the Fresnel diffraction approximation. The fitting determines the photothermal phase shift, the photothermal quantum yield, the temperature change of the optical path, and the thermal diffusivity. We study two semiconductors: Gallium Arsenide and Silicon obtaining good agreement with previously reported data.

1 Introduction

Photothermal refers to techniques that monitor the material properties changes in material properties due to the heat resulting from light photons' absorption. The thermoelastic effect produces volume variations inducing deformations of the sample's surface and changes in the refraction index's bulk values. Surface's deformation gives rise to photothermal mirror (PTM) techniques [1–7]. Pump light's absorption induces a nanometric bump or surface's deformation thanks to photoelasticity [8, 9]. Analysis of the diffraction pattern of a probe beam reflected by the affected surface yields a signal proportional to the induced photothermal phase shift. Marcano has recently reported the use of this method to measure the photothermal quantum yields (PTQY) of semiconductors, namely the ability of the sample to generate heat upon interaction with light [10]. On the other hand, the refraction index and volume changes induce a phase shift of a probe light transmitted through the sample. Affected diffraction pattern yields the photothermal lens (PTL) signal. The PTM signal is proportional to the thermoelastic coefficient. In contrast, the PTL signal is proportional to the optical path's thermal change, which includes thermoelastic pathlength changes and the thermal gradient of the refraction index. Both, PTM and PTL contributions are proportional to the PTQY. Semiconductors thermal coefficient for the optical path and PTQY values are not readily available in the open literature. However, these values are crucial for evaluating a semiconductor for possible photothermal or photoelectrical applications. Combined PTL and PTM experiments result in a complete photothermal characterization of the sample. In this work, we conduct PTM and PTL Z-scan experiments to characterize two common semiconductors—Silicon (Si) and Gallium Arsenide (GaAs). In the experiments, we keep the sample's position fixed. A lens focuses the excitation beam onto the semiconductor piece. As a pump beam, we use the light from a diode-pumped solid-state (DPSS) laser at 532 nm. We scan the lens along the longitudinal direction generating different spot sizes. A highly collimated probe beam hits the same sample's spot. The probe beam spot diameter is much larger than the pump beam one, corresponding to a highly mode-mismatched configuration. Since the sample is not moving, the chosen configuration simplifies the alignment procedure and the data's interpretation.

✉ Aristides Marcano Olaizola
amarcano@desu.edu

[1] Division of Physics, Engineering, Mathematics, and Computer Science, Delaware State University, 1200 North DuPont Highway, Dover, DE 19901, USA

[2] Unidad Profesional Interdisciplinaria en Ingeniería Y Tecnologías Avanzadas, Av. Instituto Politécnico Nacional No 2580, Col. Barrio La Laguna Ticomán, Del. Gustavo A. Madero, Mexico City, México

As probe light in the PTL experiment, we use the radiation from a DPSS laser at 1064 nm. The semiconductor partially transmits the near-infrared (NIR) probe light. A NIR detector analyzes the far-field diffraction patterns of the transmitted probe beam. In the PTM set-up, we use the light from a CW He–Ne laser at 632 nm. Scanning the pump focusing lens, we produce a single-peak Z-scan signature. The fitting of the Z-scan response using well-established diffraction theory models yields the induced phase-shift value [7, 10–14]. The combined analysis of the PTM and PTL Z-scan curves provides the value of the PTQY and the thermal coefficient of the optical path for Si and GaAs. By studying the time dependence of the signals, we confirm the samples' thermal diffusivity values.

2 Theoretical considerations

The concurrent resolution of the thermal diffusivity equation and the equation for the photo-elastic deformations for the temperature changes due to the absorption of a Gaussian beam provides the PTM and PTL theoretical models [10–15]. The absorption of the pump light injects heat onto the bulk of the sample. The heat induces local thermoelastic deformations, and changes in the refraction index giving rise to local PTM and PTL effects. Thermal diffusivity acts as a compensation mechanism by spreading the heat in the sample. Over time, a stationary distribution of the temperature establishes. The PTL affects the wavefront of the transmitted probe beam while the surface thermal bump yields the PTM signal. The Fresnel diffraction theory gives the value of the field at the detection plane. We measure the transmission of the reflected probe beam through a small aperture located at the far-field and centered on the beam's central spot. The slit's dimension is much smaller than the radius of the probe beam. Thanks to this fact, it is enough to calculate the field at the probe beam spot center. Thus, the signal is

$$W(z,t) = \frac{I(z,t) - I_o}{I_o}, \tag{1}$$

where [12, 13]

$$I(z,t) = I_{oo}\left|\int_0^\infty \exp(-(1+iV)g - i\Phi(g,z,t)dg\right|^2, \tag{2}$$

is the intensity of the probe light at the center of the beam spot; I_o is the intensity of the probe light in the absence of the pump beam, I_{oo} is a constant, $V = z_o/z_p + z_p[(z_o/z_p)^2 + 1]/d$ is the Fresnel parameter, z_o is the distance from the probe beam waists to the sample, z_p is the Rayleigh range of the probe beam, and d is the distance from the sample to the detection plane, $\Phi(g,z,t)$ is the photothermal phase shift. We consider the pump beam to be Gaussian with Rayleigh range z_e. The induced PTL phase shift is [12, 13]

$$\Phi_{PTL}(r,z,t) = \Phi_{\text{oPTL}}\int_1^{1/(1+2t/t_c(z))} \frac{1-\exp(-2xm(z)r)}{2x}\,dx \tag{3}$$

where

$$\Phi_{oPTL} = \Psi P_{ePTL}(1-R)(dS/dT)/(k\lambda_p) \tag{4}$$

is the PTL phase-shift amplitude, $m(z) = a_p^2/a_e^2(z)$ is the mode-matching parameter, a_p is the beam radius of the probe beam, $a_e(z) = a_{eo}\sqrt{1+z^2/z_e^2}$ is the pump beam radius, a_{eo} is the pump beam radius at the waist, λ_p is the probe beam wavelength, P_{ePTL} is the power of the pump light used in the PTL experiment, R is the sample's reflectance, κ is the sample's thermal conductivity, r is the transversal coordinate, t is the time of the signal detection, $t_c(z) = a_e^2(z)/(4D)$ is the thermal mirror build-up time, D is the thermal diffusivity coefficient, and ψ is the fraction of the absorbed light energy converted into heat or PTQY. dS/dT is the temperature coefficient of the optical pathlength, Andrade et al. have calculated [15]

$$\frac{dS}{dT} = (1+\nu)(n-1)\alpha + \frac{1}{4}\alpha n^3 Y(\sigma_{11}+\sigma_{22}) + \frac{dn}{dT}, \tag{5}$$

where ν is the Poisson's ratio, α is the linear expansion coefficient, Y is the Young modulus, n is the refractive index, σ_{11} and σ_{22} are the stress-optic coefficients, and dn/dT is the refractive index change with temperature. Values of this parameter for doped glasses used in solid-state laser manufacturing has been widely published [15–17]. However, the values of dS/dT for semiconductors are generally unknown.

The PTM induced phase shift is

$$\Phi_{PTM}(g,z,t) = \Phi_{oPTM}\int_0^\infty \exp\left(-\eta^2/8\right) f(\eta,z,t) J_o\left(\eta\sqrt{gm(z)}\right)d\eta, \tag{6}$$

where

$$f(\eta,z,t) = \frac{\eta t}{t_c(z)} Erfc\left(\eta\sqrt{\frac{t}{4t_c(z)}}\right) - 2\sqrt{\frac{t}{\pi t_c(z)}}\exp\left(-\eta^2\frac{t}{4t_c(z)}\right) + \frac{2}{\eta}Erf\left(\eta\sqrt{\frac{t}{4t_c(z)}}\right), \tag{7}$$

$$\Phi_{oPTM} = -P_{ePTM}\cdot(1-R)\cdot\psi\cdot\alpha\cdot(1+\nu)/\left(\lambda_p\kappa\right), \tag{8}$$

J_o is the Bessel function of zero order, λ_p is the probe beam wavelength, and P_{ePTM} is the pump power used in the PTM experiment.

The fitting of the PTL and PTM Z-scan experiments provide the phase amplitudes Φ_{oPTM} and Φ_{oPTL}, respectively. Dividing Eq. (8) over Eq. (4), we obtain the relation

$$\frac{-\Phi_{oPTM}}{\Phi_{oPTL}} = \frac{\alpha \cdot (1+\nu)}{dS/dt}\left(\frac{P_{ePTM}}{P_{ePTL}}\right), \tag{9}$$

Using Eq. (9) we can estimate the value of dS/dT if the parameters α and ν are known.

The second term in Eq. (5) is generally negligible [15]. We determine the value dn/dT from the value of dS/dT using the approximate relation

$$\frac{dn}{dT} \cong \frac{dS}{dT} - (1+\nu)(n-1)\alpha. \tag{10}$$

We can estimate the value of the PTQY ψ from Eq. (4). Using this value and Eq. (8) we determine the value of dS/dT.

The PTM and PTL signals have a similar time evolution regulated by the time build-up t_c. This time is inversely proportional to the thermal diffusivity coefficient D. By analyzing the signal's time dependence, we confirm the value of D. The analysis shows that this parameter is the same for both PTM and PTL situations.

3 Experiment

Figure 1 shows a schematic of the experimental set-up for combined PTM and PTL experiments. A 200-mW DPSS laser provides the pump light at 532 nm. Lenses L_1 and L_2 collimate the pump light up to a diameter of 5 mm. We use an optical chopper to modulate the pump beam. A small beam-splitter B_1 selects part of this light and redirects it to the reference detector D_R. Rectangular prism P_1 reflects the pump light toward the focusing lens L_3. Scanning of this lens along the longitudinal direction Z produces different pump beam spots on the sample yielding the Z-scan response. The sample remains in a fixed position during the scanning procedure. A 2-mW He–Ne laser at 632-nm provides the probe beam for the PTM experiment. Lenses L_4 and L_5 collimate this probe beam up to a diameter of 6 mm. The mirror M_1 reflects this light toward the sample. The mirror M_3 redirects the reflected probe light toward the aperture A_1 and then to the semiconductor detector D_{S1} that provides the PTM signal. The detector sends the signal to a current amplifier and then to a digital oscilloscope for processing. A separate DPSS laser working at 1064-nm gives the probe beam for the PTL experiment. Lenses L_6 and L_7 collimate this second probe light up to a diameter of 6 mm. The mirror M_2 redirects this light toward the sample. The NIR passes through it thanks to the NIR semi-transparency of the semiconductor wafers. The light passes through the aperture A_2 before hitting the secondary signal detector that provides the PTL signal. The signal goes then to the amplifier and finally to the digital oscilloscope.

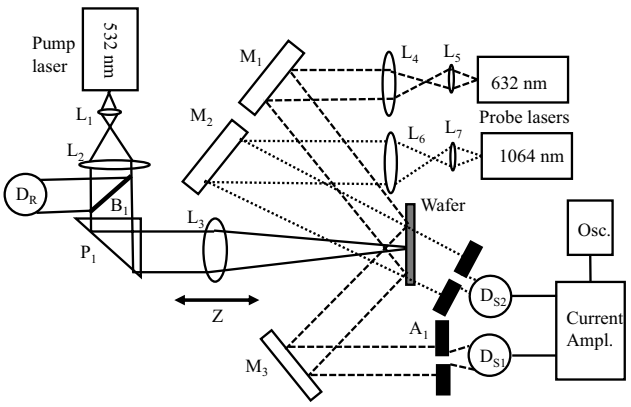

Fig. 1 Experimental set-up for conducting combined PTM and PTL experiments consisting of a DPSS pump laser at 532-nm, collimating lenses L_1 and L_2, an optical chopper, reference detector D_R, beam splitter B_1, a reflecting prism P_1, a focusing lens L_3, probe lasers He–Ne at 632-nm and DPSS 1064-nm, collimating lenses L_4, L_5, L_6 and L_7, mirrors M_1, M_2, and M_3, apertures A_1 and A_2, semiconductor detectors D_{S1} and D_{S2}, a current amplifier, and a digital oscilloscope

Detector arrays can be used as an alternative to registering the signal allowing a full 2D transmission/reflection image for thermal analysis. However, for our experiments, a simple diode detector placed at the center of the beam spot is good enough for the analysis considering that the theoretical model refers to calculating the probe beam intensity at this point. This basic detection method provides a good signal-to-noise ratio even for pump powers below 10 mW.

The samples are double-side polished wafers of Silicon (Si) and Gallium Arsenide (GaAs) of 4-cm radius and thickness of 0.7 and 0.56 mm, respectively (Universal Wafers, Inc.). The pump beam focusing does not generate damage over the wafers' surface thanks to its limited power. In Table 1, we show the characteristic thermal and optical parameters of GaAs and Si taken from the available literature.

Table 1 Thermal and optical characteristics of Si and GaAs

Parameter	Silicon	GaAs
Thermal diffusivity D ($cm^2\ s^{-1}$)	0.31 [18]	0.9 [18]
Thermal conductivity κ ($W\ cm^{-1}\ ^oK^{-1}$)	0.55 [18]	1.59 [18]
Thermoelastic coefficient α (K^{-1})	5.75 10–6 [18]	2.6 10^{-6} [18]
Poisson ratio	0.22 [19]	0.31 [19]
Refraction index at 532 nm	4.15 [20]	4.13 [20]
Reflectance at 532-nm	0.37 [20]	0.37 [20]

The semiconductors exhibit absorption at the probe wavelength of 1064-nm. We note that the 1064-nm absorption is much smaller than the absorption at visible wavelengths, for which the semiconductors are virtually opaque. The probe absorption generates some heat. However, this heat does not affect the results since we measure the relative change of the probe beam's profile when the pump beam is modulated. This procedure automatically cancels any possible contribution to the signal from the probe beam. On the other hand, we collimate the probe beam to a diameter much larger than the pump beam diameter. It means that the probe beam's heat is nearly uniformly distributed over the region affected by the focused pump beam, resulting in negligible PTL effects. Experiments confirm that the probe beam does not produce any contribution. There is no signal when the pump beam is absent, even in the probe beam's presence.

We record the Z-scan signal by scanning the lens L_3 while keeping the position of the sample fixed. Under this configuration, the Z-scan response is single peaked. The maximal value takes place at maximal focusing. The design simplifies the alignment procedure and the interpretation of the data. We estimate the signal using Eq. 1, and the induced phases using Eqs. 3 and 6 for the PTL and PTM data, respectively. The fitting provides the value of the induced PTL and PTM phase shifts.

4 Results and analysis

The experiments show that the PTM signal is negative, while the PTL one is positive. Figure 2a shows the AC components of the PTM and PTM signals from the GaAs wafer when using a 532-nm pump light. For the PTM experiment, we use a probe at 632 nm, while for the PTL results, a DPSS 1064-nm laser provides the probe beam. The chopper modulates the pump at 100 Hz for the GaAs experiments, while for the Si we use a frequency of 200 Hz. For comparison, we have plotted the modulated pump signal. When the pump is on, the PTM signal decreases while the PTM one increases. When the pump is off, the PTM recovers, and the PTM decreases. The surface distortion's intrinsic shape produces a decrease of intensity at the center of the reflected probe beam diffraction pattern in the far-field. The effect on the transmitted probe field is positive due to the positive value of the constant dS/dT. Figure 2b confirms a similar feature for the Si wafer.

The signal's amplitude depends on the modulation frequency and the lens's z-position. The theoretical model includes these effects as dependences on time t and focal lens position z, respectively. We generate Z-scan curves for different times defined by the frequency of modulation. The model includes several parameters such as d, z_o, and z_p. However, these parameters are fixed for all experiments and are easily defined by the configuration. The Z-scan signature's amplitude and width give the phase-shift amplitude (Φ_{oPTL} or Φ_{oPTM}) and the pump field Rayleigh range (z_e), respectively. These two values are the only parameters we fit in the analysis.

Figure 3a shows the PTM Z-scan of the GaAs wafer generated by scanning the focusing lens near the focus position. We use a pump power of 96 mW to generate the result. Using the chopper, we modulate the pump at 50, 100, and 200 Hz. As expected, the signal decreases as the modulation frequency increases. The solid lines are the fitting of the experimental data calculated using the Eqs. (1), (2), (6), and (7) with the parameters $\lambda_p = 632$ nm, $\lambda_e = 532$ nm, $z_p = 2700$ cm, $z_o = 0$, $z_e = 0.014$ cm, d = 161 cm, $D = 0.31$ cm^2s^{-1}, $\phi_{oPTM} = -0.012$, $n_{GaAs} = 4.13$, and times $t = 10$, 5 and 2.5 ms, corresponding to the frequencies 50, 100, and 200 Hz, respectively. The parameters λ_p, λ_e, d, and t are fixed by the conditions of the experiments. The parameter D and n_{GaAs} are from Table 1. We fit the values of z_p, z_e, and ϕ_{oPTM} until we achieve a good agreement between theory and experiments. Figure 3b shows the GaAs' PTL experiments modulating the pump at 50, 100, and 200 Hz. The signal is about one order of magnitude larger than the PTM one. We reduce the power, so the response had a value comparable to the PTM signal. We use a power of 10.27 mW.

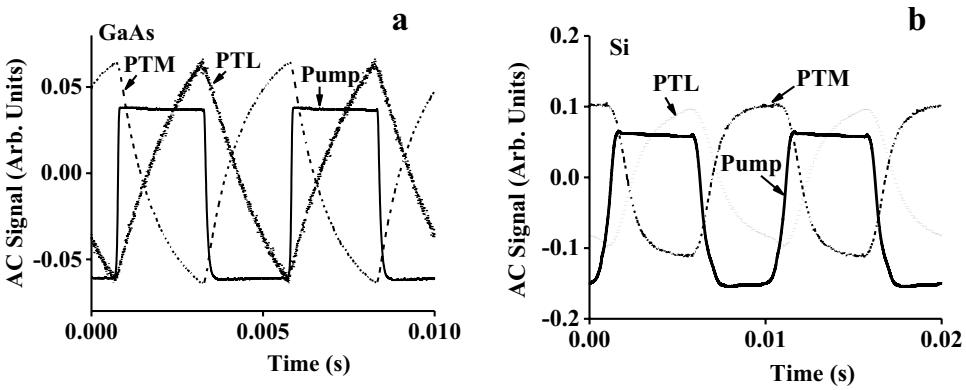

Fig. 2 Time dependence of the AC component of the PTM (slash lines) and the PTL (dotted lines) signals for GaAs (**a**) and Si (**b**). For comparison we have also plotted the modulated pump beam (solid lines)

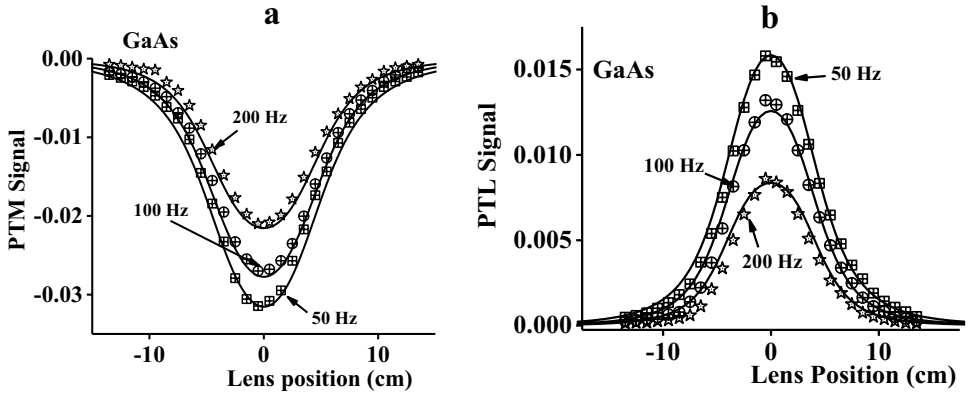

Fig. 3 **a** PTM Z-scan signal of GaAs obtained at modulation frequencies 50, 100, and 200 Hz at 96 mW of pump 532-nm radiation. The solid lines correspond to the theoretical fitting using Eqs. (1), (2), (6), and (7) and parameters $\lambda_p = 632$ nm, $\lambda_e = 532$ nm, $z_o = 0$, $z_p = 2700$ cm, $z_e = 0.014$ cm, $d = 161$ cm, $D = 0.31$ cm^{2}s^{-1}, $\phi_{oPTM} = -0.012$, $n_{GaAs} = 4.13$, and times $t = 10$, 5 and 2.5 ms for frequencies 50, 100, and 200 Hz, respectively. **b** PTL Z-scan signal of GaAs obtained at modulations frequencies 50, 100, and 200 Hz and 10 mW of the 532-nm pump radiation. The solid lines correspond to the theoretical fitting using Eqs. (1), (2), (3), and (4) and parameters $\lambda_p = 1064$ nm, $\lambda_e = 532$ nm, $z_o = 0$, $z_p = 2700$ cm, $z_e = 0.014$ cm, $d = 118$ cm, $D = 0.31$ cm^{2}s^{-1}, $\phi_{oPTL} = -0.013, = 4.13$, and times $t = 10$, 5 and 2.5 ms, for frequencies 50, 100, and 200, respectively

The solid lines correspond to the theoretical fitting obtained by solving Eqs. (1), (2), (3), and (4) with the parameters, $d = 118$ cm, and $\phi_{oPTL} = 0.013$. The rest of the parameters are as in Fig. 3a. Using Eq. (8), Table 1, and the measured value of ϕ_{oPTM}, we estimate the PTQY for GaAs as $\psi_{\mathrm{GaAs}} = 0.92$. Using this value, the measured value ϕ_{oPTL}, and Eq. (9), we obtain for GaAs dS/dT = 1.24 10^{-4} ^{o}K^{-1}. Using Eq. (10) and Table 1, we estimate for GaAs $dn/dT = 1.01$ 10^{-4} ^{o}K^{-1}.

Figure 4 describes the results for the Si wafer. Figure 4a shows the Si PTM Z-scan response obtained using a pump power of 144 mW at modulation frequencies 100, 500, and 1000 Hz. The evolution occurs faster thanks to a larger value of the Si thermal diffusivity coefficient. The signal is about one order of magnitudes smaller than the signal for GaAs for similar power levels. The solid lines are the fitting of the experimental data calculated using the Eqs. (1), (2), (6), and (7) with the parameters $\lambda_p = 1064$ nm, $\lambda_e = 532$ nm, $z_o = 0$, $z_p = 2700$ cm, $z_e = 0.014$ cm, $d = 161$ cm, D = 0.9 cm^{2}s^{-1}, $\phi_{oPTM} = -0.0022$, $n_{Si} = 4.15$, and times $t = 5$, 1, and 0.5 ms, corresponding to the frequencies 100, 500, and 1000 Hz, respectively. The conditions of the experiment give the parameters λ_p, λ_e, d, and

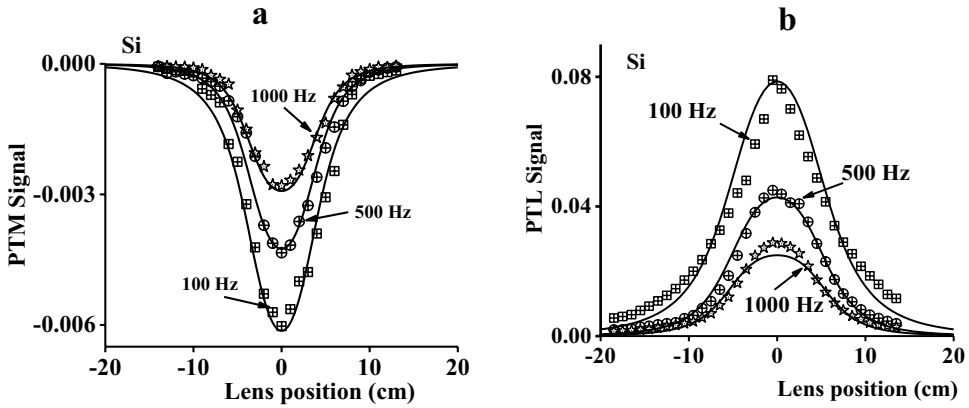

Fig. 4 **a** PTM Z-scan signal of Si obtained at modulation frequencies 100, 500, and 1000 Hz at 144 mW of pump 532-nm radiation. The solid lines correspond to the theoretical fitting using Eqs. (1), (2), (6), and (7) and parameters $\lambda_p = 632$ nm, $\lambda_e = 532$ nm, $z_o = 0$, $z_p = 2700$ cm, $z_e = 0.014$ cm, $d = 161$ cm, $D = 0.9$ cm^{2}s^{-1}, $\phi_{oPTM} = -0.0022$, $n_{Si} = 4.13$, and times $t = 10$, 5 and 2.5 ms for frequencies 50, 100, and 200 Hz, respectively. **b** PTL Z-scan signal of Si obtained at modulations frequencies 50, 100, and 200 Hz at 158 mW of 532-nm pump radiation. The solid lines correspond to the theoretical fitting using Eqs. (1), (2), (3), and (4) and parameters $\lambda_p = 1064$ nm, $\lambda_e = 532$ nm, $z_o = 0$, $z_p = 2700$ cm, $z_e = 0.014$ cm, $d = 118$ cm, $D = 0.9$ cm^{2}s^{-1}, $\phi_{oPTL} = 0.06$, $n_{Si} = 4.13$, and times $t = 10$, 5 and 2.5 ms, for frequencies 50, 100, and 200, respectively

Table 2 Measured photothermal parameters of Si and GaAs

Parameter	Si	GaAs
PTQY (ψ) at 532 nm	0.75	0.92
dS/dT [°K^{-1}]	$+1.31\ 10^{-4}$	$+1.24\ 10^{-4}$
dn/dT [°K^{-1}]	$+1.21\ 10^{-4}$	$+1.01\ 10^{-4}$

t. The parameters D and n_{Si} are taken from Table 1. We fit the values of z_p, z_e, and ϕ_{oPTM} until we achieve a good agreement between theory and experiments. Figure 4b shows similar results for the Si PTL Z-scan obtained using 158 mW of the 532-nm radiation.

The PTL signal is again about one order of magnitude larger than the PTM one. The solid lines correspond to the fitting of the experiments by resolving Eqs. (1), (2), (3), and (4) with the parameters $\phi_{oPTL}=0.06$, $d=118$ cm and $D=0.9$ cm^2/s. The rest of the parameters are as in Fig. 4a. Using Eq. (8), Table 1, and the measured value of ϕ_{oPTM}, we estimate the PTQY for Si as $\psi_{Si}=0.75$. Using this value, the measured value $\phi_{oPTL,}$ and Eq. (9), we obtain for Si $dS/dT=1.31\ 10^{-4}$ °K^{-1}. Using Eq. (10) and Table 1, we estimate for Si $dn/dT=1.21\ 10^{-4}$ °K^{-1}.

Table 2 summarizes all the characteristics found in this study.

5 Conclusions

We develop a combined PTL and PTM Z-scan method to estimate the PTQY and the GaAs and Si wafers' photothermal parameters. We conduct experiments with fixed samples' positions. The scanning of the lens, focusing the pump beam, yields the Z-scan signature. The configuration facilitates the alignment procedure and the interpretation of the results. We show that the PTM experiments produce a negative signal, while the PTL configuration yields a positive one. The PTL signal is about one order of magnitude larger than the PTM one. We fit the experiments using a Fresnel diffraction model previously developed for both types of experiments. We found a good agreement between predictions of the theory and the experimental observations. We obtain the values for the PTQY, the parameters dS/dT and dn/dT for both semiconductors.

Acknowledgements The authors acknowledge the National Science Foundation support of the present research (Awards 831332 and 1719379). Luna Sánchez acknowledges support from the Mexican Agency CONACYT.

References

1. N.G.C. Astrath, L.C. Malacarne, P.R.B. Pedreira, A.C. Bento, M.L. Baesso, J. Shen, Time-resolved thermal mirror for nanoscale surface displacement detection in low absorbing solids. Appl. Phys. Lett. **91**, 191908 (2007)
2. F. Sato, L.C. Malacarne, P.R.B. Pedreira, M.P. Belancon, R.S. Mendes, M.L. Baesso, N.G.C. Astrath, J. Shen, Time-resolved thermal mirror method: A theoretical study. J. Appl. Phys. **104**, 053520 (2008)
3. L.C. Malacarne, F. Sato, P.R.B. Pedreira, A.C. Bello, R.S. Mendes, M.L. Baesso, N.G.C. Astrath, J. Shen, Nanoscale surface displacement detection in high absorbing solids by time-resolved thermal mirror. Appl. Phys. Lett. **92**, 131903 (2008)
4. L.C. Malacarne, N.G.C. Astrath, G.V.B. Lukasievicz, E.K. Lenzi, M.S. Baesso, S. Bialkowski, Time-resolved thermal lens and thermal mirror spectroscopy with sample-fluid heat coupling: A complete model for material characterization. Appl. Spectros. **65**(1), 99–104 (2011)
5. V.S. Zanuto, L.S. Herculano, M.S. Baesso, G.V.B. Lukazievicz, C. Jacinto, L.C. Malacarne, N.G.C. Astrath, Thermal mirror spectrometry: an experimental investigation of optical glasses. Opt. Mat. **35**, 1129–1133 (2013)
6. N.G.C. Astrath, L.C. Malacarne, V.S. Zanuto, M.P. Belancon, R.S. Mendes, M.L. Baesso, C. Jacinto, Finite size effect on the surface deformation thermal mirror method. J. Opt. Soc. Am. B **28**(7), 1735–1739 (2011)
7. G.V.B. Lukasievicz, L.C. Malacarne, N.G.C. Astrath, V.S. Zanuto, L.S. Herculano, S.E. Bialkowski, A theoretical and experimental study of time-resolved thermal mirror with non-absorbing heat-coupling fluids. Appl. Spectrosc. **66**(12), 1461–1467 (2012)
8. P. Kuo, M. Munidasa, Single-beam interferometry of a thermal bump. Appl. Opt. **29**(36), 5326–5331 (1990)
9. B. Li, Z. Zhen, S. He, Modulated photothermal deformation in solids. J. Phys. D: Appl. Phys. **24**(12), 2196–2201 (1991)
10. A. Marcano, Photothermal mirror Z-scan spectrometry of opaque samples. J. Opt. Soc. Am. B **36**(10), 2907–2912 (2019)
11. A. Marcano, G. Gwanmesia, B. Workie, Photothermal mirror method for the study of thermal diffusivity and thermo-elastic properties of opaque solid materials. Intern. J. Thermophys. **38**, 136 (2017)
12. A. Marcano, N. Melikechi, In: *Thermal Wave Physics and Related Photothermal Techniques: Basic Principles and Recent Developments*, ed. by E. Marin. Pump-probe mode-mismatched photothermal lens spectroscopy in the continuous wave regime, (Transworld. Research Network, 2009), p. 287
13. A. Marcano, C. Loper, N. Melikechi, High sensitivity absorption measurement in water and glass samples using a mode-mismatched pump-probe thermal lens method. Appl. Phys. Lett. **78**, 3415–3417 (2001)
14. A. Marcano, C. Loper, N. Melikechi, Pump probe mode mismatched Z-scan. J. Opt. Soc. Am. B **19**, 119–124 (2002)
15. A.A. Andrade, T. Catunda, I. Bodnar, J. Mura, L. Baesso, Thermal lens determination of the temperature coefficient of optical path length in optical materials. Rev. Sci. Instrum. **74**(1), 877–880 (2003)
16. W. Koechner, *Solid- State Laser Engineering*, vol. 01 (Spring, New York, 1988)
17. Casix, JDS Uniphase Company. http://www.casix.com
18. S.M. Sze, K.Ng. Kwok, *Physics of Semiconductor Devices*, 3rd edn. (John Wiley & Sons, Inc., 2007)
19. S.M. Sze, *Semiconductor Sensors*, Appendix D, (Wiley, 1994), p. 535
20. J.B. Theeten, D.E. Aspnes, R.P.H. Chang, A new resonant ellipsometric technique for characterizing the interface between GaAs and its plasma-grown oxide. J. Appl. Phys. **49**, 6097 (1978)